

Entropy-Based Evidence for Bitcoin's Discrete Time Mechanism

Bin Chen*

School of Electronics and Information Engineering,
Shenzhen University
bchen@szu.edu.cn

Pan Feng

School of Electronics and Information Engineering,
Shenzhen University

Abstract—Bitcoin derives a verifiable temporal order from probabilistic block discovery and cumulative proof-of-work rather than from a trusted global clock. We show that block arrivals exhibit stable exponential behavior across difficulty epochs, and that the proof-of-work process maintains a high-entropy search state that collapses discretely upon the discovery of a valid block. This entropy-based interpretation provides a mechanistic account of Bitcoin's non-continuous temporal structure. In a distributed network, however, entropy collapse is not completed instantaneously across all participants. Using empirical observations of temporary forks, we show that collapse completion unfolds over a finite propagation-bounded interval, while remaining rapid in practice.

Index Terms—Non-continuous time, entropy collapse, difficulty adjustment, proof-of-work.

I. INTRODUCTION

A key challenge in decentralized systems is establishing a reliable notion of time without centralized clocks. Chen [1] proposed that Bitcoin addresses this challenge by advancing time through stochastic block discoveries rather than through an external timeline, and introduced the concept of entropy collapse to describe the discrete resolution of uncertainty at block discovery. While this framework clarifies the conceptual structure of Bitcoin's non-continuous time, it has not yet been supported by large-scale empirical analysis. This paper fills that gap using real-world block arrival observations.

Existing studies of Bitcoin block timing largely focus on characterizing arrival statistics or measuring network effects in isolation. Early work established that proof-of-work produces approximately exponential inter-arrival times and highlighted the impact of network propagation delay on forks and stale blocks [2], [3]. Subsequent analyses refined statistical models of block arrivals and examined deviations from ideal Poisson behavior under changing network conditions [4], [5]. Separately, empirical studies of blockchain forks quantified the frequency and duration of competing blocks and attributed prolonged forks to network-level effects rather than to consensus failure [6]. These lines of work typically treat timing statistics, forks, and protocol feedback as distinct phenomena, and often regard the exponential form as an empirical regularity.

In contrast, we examine Bitcoin as a permissionless consensus system in which time cannot be assumed as an external or synchronized input. We ask whether the Poisson regime observed in block arrivals is merely incidental, or whether

it is actively sustained by protocol-level mechanisms under long-term variation in hashrate and network conditions.

We analyze approximately 425,000 observed block arrivals from 2016 to 2024 [7], spanning 211 complete difficulty epochs excluding 22 incomplete ones. Because Bitcoin does not enforce strict global clock synchronization, block header timestamps are only loosely constrained and may differ across miners. We therefore use arrival times observed at single nodes as a consistent measurement basis. Using these data, we examine waiting-time distributions, epoch-level rates, autocorrelations, and interval entropy.

Our analysis makes three empirical contributions. First, we demonstrate epoch-level exponential stability. Waiting times remain well-approximated by an exponential form across difficulty epochs, and estimated arrival rates stay near the protocol target over long horizons. Second, we show that discovery entropy concentrates in the high-entropy region of each interval. This indicates that blocks are typically found while uncertainty remains substantial. Third, we quantify distributed completion of entropy collapse using the survival function of fork durations. Most forks resolve rapidly, while a nonzero tail reflects propagation-bounded completion.

The paper is structured as follows. Section II develops the theoretical foundations of Bitcoin's temporal dynamics. Section III provides empirical evidence for exponential arrivals and epoch-level stability. Section IV analyzes interval-level entropy, its collapse at block discovery, and its implications for discrete temporal progression. Section V concludes.

II. THEORETICAL FRAMEWORK FOR BITCOIN'S DISCRETE TEMPORAL DYNAMICS

This section formalizes a systems-level description of Bitcoin's temporal dynamics using three components. First, proof-of-work is modeled as Bernoulli sampling in a vast hash space, which yields the Poisson arrival limit for block discovery. Second, interval-level uncertainty is quantified by entropy and is resolved at discovery, providing a discrete notion of temporal advancement at the level of observation. Third, difficulty adjustment is expressed as a feedback rule that regulates the rate of these discrete events across epochs.

Together, these elements define the theoretical structure that will be tested empirically in the following sections.

A. Bernoulli Sampling, Difficulty, and the Poisson Arrival Limit

Bitcoin's proof-of-work mechanism operates through an immense number of independent Bernoulli trials. Each hash attempt succeeds if its output lies below the target threshold T_{target} , which is determined by the difficulty parameter

$$D = \frac{T_0}{T_{\text{target}}}. \quad (1)$$

where T_0 is a fixed reference target corresponding to difficulty one in the Bitcoin protocol. As difficulty increases, the admissible hash region contracts and the per-trial success probability becomes

$$\theta = \frac{1}{D \cdot 2^{32}}. \quad (2)$$

Let H denote the global hashrate. By time t the network performs $N(t) = \lfloor Ht \rfloor$ independent trials, yielding the survival probability

$$\Pr[T > t] = (1 - \theta)^{N(t)}. \quad (3)$$

Bitcoin operates in the classical rare-event regime where $\theta \rightarrow 0$, $N(t) \rightarrow \infty$, and $\theta N(t)$ remains finite. Taking this joint limit gives [8]

$$\Pr[T > t] \rightarrow e^{-\lambda t}, \quad \lambda = H\theta \approx \frac{H}{D \cdot 2^{32}}. \quad (4)$$

Thus T is asymptotically exponential with rate λ , and block arrivals follow a Poisson process. Since the per-trial success probability is set by the difficulty target, this relation implies the hashrate estimator

$$H \approx \frac{1}{\theta \mathbb{E}[T]} \approx \frac{D 2^{32}}{\mathbb{E}[T]}. \quad (5)$$

The Poisson limit remains valid in the presence of multiple miners because their search processes are effectively independent. Each miner constructs distinct candidate block headers through transaction selection, ordering, coinbase data, and nonce structure, thereby exploring a local possibility space Ω_m . Because each miner samples only a negligible fraction of the 2^{256} hash domain, the overlap between any two such spaces is vanishingly small,

$$\Pr[\Omega_i \cap \Omega_j] \approx 0 \quad (i \neq j). \quad (6)$$

The network therefore samples from an effective global space

$$\Omega = \bigcup_{m=1}^M \Omega_m, \quad (7)$$

and the time to block discovery is the minimum of M independent exponential waiting times. This minimum remains exponentially distributed with aggregate rate λ , confirming that parallel mining preserves the Poisson arrival structure.

B. Difficulty Feedback for Long-Horizon Stability

Let D_k denote the difficulty at the start of epoch k and let $T_{\text{obs},k}$ be the observed duration of that epoch. The protocol aims for an expected epoch duration of $T_{\text{epoch}} = 2016 \times 600$ s. Because the Poisson limit yields an exponential waiting time with rate λ , regulating the long-run arrival rate amounts to regulating λ across epochs under changing hashrate.

Bitcoin updates difficulty via a discrete feedback rule based on the last epoch's realized duration [9]

$$D_{k+1} = D_k \frac{T_{\text{epoch}}}{T_{\text{obs},k}}. \quad (8)$$

When blocks arrive faster than expected, $T_{\text{obs},k} < T_{\text{epoch}}$, the update increases difficulty and reduces the per-trial success probability. When blocks are slower, it decreases difficulty. This feedback stabilizes the effective arrival rate across epochs and helps sustain the exponential regime required for decentralized coordination.

C. Entropy Collapse and the Granularity of Bitcoin Time

For a fixed rate λ within an interval, the probability that a block has been discovered by time t is

$$p(t) = 1 - e^{-\lambda t}. \quad (9)$$

Let τ denote the discovery time within the interval. Under the longest-chain rule, an honest node that observes a valid block immediately abandons its ongoing search and begins the next interval from the newly adopted tip. The interval-level uncertainty collapses locally and begins to collapse network-wide,

$$H(\tau^-) > 0, \quad H(\tau^+) \rightarrow 0. \quad (10)$$

Interval-level uncertainty can be quantified by the binary entropy

$$H(t) = -p(t) \log_2 p(t) - [1 - p(t)] \log_2 (1 - p(t)). \quad (11)$$

As an inter-arrival interval progresses, this entropy evolves deterministically (unimodally). Under the longest-chain rule, an honest node that observes a valid block immediately abandons its ongoing search and begins the next interval from the newly adopted tip. The interval-level uncertainty collapses locally and begins to collapse network-wide.

$$H(t^-) > 0, \quad H(t^+) \rightarrow 0. \quad (12)$$

This entropy collapse defines the generation of protocol-level time. Let $0 < T_1 < T_2 < \dots$ denote successive block arrival times observed by an honest node and define

$$\Delta T_n = T_{n+1} - T_n. \quad (13)$$

No new temporal information is produced by the protocol during the open intervals (T_n, T_{n+1}) . Bitcoin time therefore consists of the discrete sequence of block arrival events $T = \{T_1, T_2, \dots\}$, rather than a continuous timeline.

In this sense, the granularity of Bitcoin time is not imposed externally but emerges endogenously from entropy

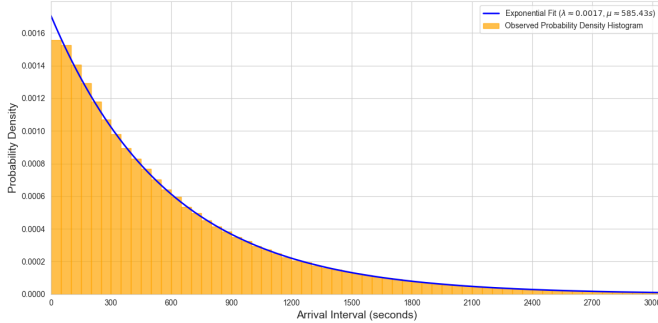


Fig. 1. Histogram of Inter-arrival Intervals with Fitted Exponential density.

accumulation and collapse. Each block discovery both resolves uncertainty and advances the system’s internal temporal state, establishing a non-continuous notion of time grounded in information resolution rather than in physical clocks.

III. EMPIRICAL DISTRIBUTION OF INTER-ARRIVAL TIMES

This section examines whether the empirical sequence of inter-arrival intervals conforms to the exponential model implied by proof of work. The analysis is based on observed block arrivals recorded from 2016 to 2024.

A. Inter-arrival Durations and Epoch Stability

Let $\Delta T_1, \Delta T_2, \dots, \Delta T_N$ denote the observed inter-arrival intervals. The sample mean is

$$\bar{\Delta T} = \frac{1}{N} \sum_{i=1}^N \Delta T_i. \quad (14)$$

Figure 1 shows the empirical histogram of ΔT_i together with the exponential density implied by the estimated rate $\hat{\lambda} = 1/\bar{\Delta T}$. The fitted distribution corresponds to a mean inter-arrival interval of 585.43 s. For visual clarity, the figure truncates inter-arrival intervals above 3000 s. Such extreme intervals are rare, and their omission does not affect the shape of the central distribution. The histogram exhibits the characteristic right-skewed form of an exponential process. Consistent with the exponential model, the sample mean and standard deviation are of comparable magnitude. These results indicate that the global inter-arrival data conform closely to the exponential benchmark.

To examine stability across epochs, we compute an epoch-level mean inter-arrival interval from block timestamp data for each 2016-block difficulty epoch. This timestamp-based measure reflects the internal timing signal used by the protocol’s difficulty adjustment mechanism.

Figure 2 shows that epoch mean inter-arrival times cluster tightly around the ten-minute target, with most values falling within 600 ± 100 seconds and a mild tendency toward shorter intervals. The horizontal reference line indicates the overall observed mean of 585.43 seconds.

This asymmetry reflects the interaction between discrete difficulty adjustment and sustained hashrate growth. Within an epoch, difficulty is fixed, so increases in network hashrate

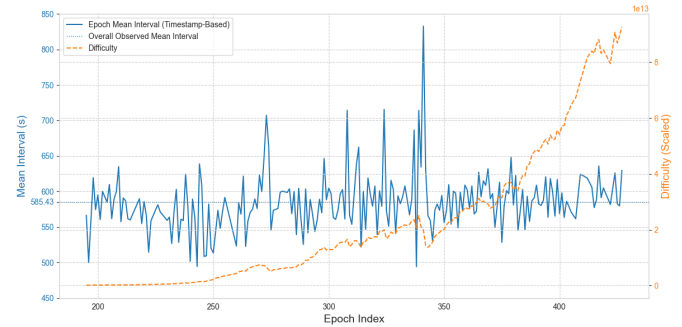


Fig. 2. Epoch-mean Inter-arrival Intervals and Contemporaneous Difficulty.

raise the effective arrival rate and bias inter-arrival intervals toward shorter values later in the epoch. The subsequent retarget reacts by increasing difficulty, but when hashrate continues to grow across epochs, the feedback operates with delay on a moving target, allowing a persistent deviation from the nominal ten-minute level.

To quantify this effect, we split each difficulty epoch into two halves of 1008 inter-arrival intervals and compute the mean duration in each half, denoted by \bar{T}_{early} and \bar{T}_{late} , respectively. Across 211 complete epochs, the late-half mean is systematically shorter than the early-half mean. Averaged over all epochs, the early-half mean is $\bar{T}_{\text{early}} = 590.08$ s, while the late-half mean is $\bar{T}_{\text{late}} = 580.78$ s, yielding an average paired difference of $\bar{T}_{\text{late}} - \bar{T}_{\text{early}} = -9.30$ s with a 95% confidence interval $[-14.80$ s, -3.81 s]. The late half is shorter in 132 out of 211 epochs (62.6%), and the paired difference is statistically significant (paired t -test $p = 0.0010$).

Because difficulty is fixed within an epoch, the mean inter-arrival time is inversely proportional to the effective hashrate. The observed bias therefore implies a gradual within-epoch increase in hashrate, with an average ratio

$$\frac{H_{\text{late}}}{H_{\text{early}}} \approx \frac{\bar{T}_{\text{early}}}{\bar{T}_{\text{late}}} \approx 1.016, \quad (15)$$

corresponding to a 1–2% increase from the early half to the late half. For comparison, the late-half mean of approximately 580 s is below the 600 s target, indicating an effective arrival rate about $600/580.78 \approx 1.033$ times faster than the protocol target on average.

Overall, these results highlight a separation of temporal scales in Bitcoin’s timekeeping mechanism. Difficulty is adjusted on a slower epoch scale through discrete feedback, constraining long-run timing behavior, while block arrivals fluctuate stochastically at the inter-arrival scale. Together, this behavior is consistent with a Poisson arrival process regulated by discrete adaptive feedback.

B. Serial Independence

If the exponential model holds, the sequence of inter-arrival intervals should exhibit no serial dependence. Autocorrelations

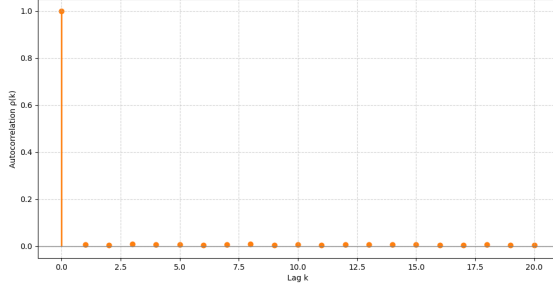


Fig. 3. Autocorrelation of Inter-arrival Intervals for Twenty Lags.

are computed using

$$\rho(k) = \frac{\sum_{i=1}^{N-k} (\Delta T_i - \bar{\Delta T})(\Delta T_{i+k} - \bar{\Delta T})}{\sum_{i=1}^N (\Delta T_i - \bar{\Delta T})^2} \quad (16)$$

for lags $k = 1, 2, \dots, 20$.

Figure 3 reports the sample autocorrelation function for the trimmed inter-arrival intervals. To reduce the influence of extreme outliers, we remove the top and bottom one percent of durations. Autocorrelations at lags 1 through 20 fluctuate tightly around zero and remain well within sampling bounds, with no detectable serial dependence. This behavior is consistent with independent exponential waiting times and a Poisson arrival process driven by independent hash attempts.

These results characterize the external timing of block arrivals observed by a participant, but they do not describe how temporal uncertainty accumulates within an interval or how it resolves at discovery. To capture these internal dynamics, Section IV introduces an interval-level entropy measure and shows how collapse events define the discrete temporal progression of the system.

IV. INTERVAL-LEVEL ENTROPY AND COLLAPSE

Entropy provides an internal representation of uncertainty within each block interval. While the arrival probability $p(t)$ increases monotonically, the corresponding binary entropy $H(t)$ follows a concave profile, peaking at $p(t) = 1/2$ and remaining elevated over much of the interval [10]. For Bitcoin’s target interval of approximately 600 seconds, this high-entropy regime is reached well before the expected block arrival, indicating that substantial uncertainty persists throughout most of the interval.

As formalized in [1], collapse completion occurs only upon block discovery. Under the longest-chain rule, an honest node that observes a valid block immediately abandons its ongoing search and begins the next interval from the newly adopted tip. This discrete reduction of uncertainty constitutes entropy collapse and defines the advancement of Bitcoin’s non-continuous time.

Building on this framework, we evaluate the entropy of each observed block interval at its realized duration using a global mean arrival rate estimated from the full sample. Figure 4 shows the resulting entropy distribution. The histogram is sharply

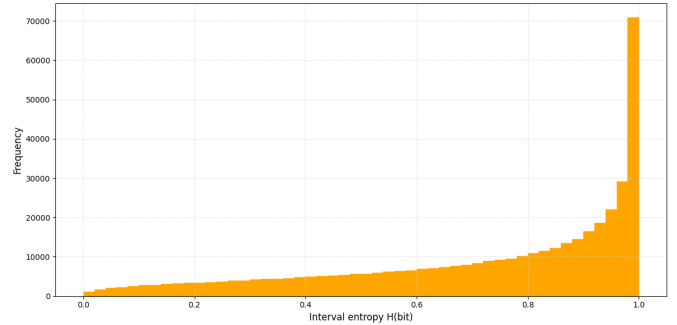


Fig. 4. Histogram of Entropy at Block Discovery

concentrated near the maximal entropy region, indicating that most block intervals terminate while uncertainty remains high. Only a small fraction of unusually short or long intervals appear in the low-entropy tails.

This empirical pattern provides direct observational support for the entropy-collapse mechanism, showing that block intervals typically terminate while uncertainty remains high and that entropy collapse is initiated by the discrete occurrence of a valid proof-of-work solution rather than by gradual probabilistic resolution. From an informational perspective, each block discovery terminates one interval and initiates the collapse of the uncertainty accumulated since the previous block. The evolution of this uncertainty within an interval is governed by the block arrival rate, which determines how rapidly entropy accumulates over time and is the statistical quantity estimated and regulated by the difficulty-adjustment mechanism.

Crucially, in a distributed network this collapse is not completed instantaneously. While entropy collapse is initiated locally at block discovery, residual uncertainty may persist across the network due to propagation delays and competing discoveries. The completion of entropy collapse therefore unfolds over a finite, propagation-bounded interval, giving rise to temporary forks and distributed resolution.

A. Distributed Completion of Entropy Collapse

In a distributed network, entropy collapse unfolds as a process rather than as an instantaneous event. Because nodes do not observe block discoveries simultaneously, collapse proceeds through a propagation-bounded completion phase during which multiple candidate blocks may temporarily coexist. When multiple valid blocks are discovered at the same height within this window, each represents a local realization of collapse, while global uncertainty persists until one branch dominates through cumulative work and the longest-chain rule [2]. Temporary forks thus provide an observable manifestation of the distributed completion of entropy collapse, rather than a breakdown of consensus.

To quantify this completion phase, we define the fork duration as the time interval between the first observed valid block at a given height and the last competing block observed before convergence to a single branch. Fork duration measures how long residual uncertainty persists after collapse is initiated.

It is distinct from block inter-arrival time, which characterizes the spacing of successive accepted blocks on the canonical chain. Fork duration thus provides an observable proxy and a lower bound on collapse completion time, as latent propagation delays or unseen orphan blocks may extend the true collapse completion process beyond what is directly measurable.

Empirically, fork durations are analyzed using the survival function

$$\hat{S}(\tau) = \Pr(\mathcal{D} \geq \tau) = \frac{1}{N} \sum_{i=1}^N \mathbf{1}(\mathcal{D}_i \geq \tau), \quad (17)$$

where \mathcal{D} denotes the fork-duration random variable, $\{\mathcal{D}_i\}_{i=1}^N$ are observed realizations of \mathcal{D} , and $\tau \geq 0$ denotes a duration threshold measured as elapsed time since the initiation of a fork.

Using the publicly available fork dataset collected via direct network monitoring [6], Figure 5 plots the empirical survival function of fork durations on a log–log scale. Consistent with prior measurements, fork events are rare and form a sparse sequence ordered by blockchain height rather than a temporally contiguous time series, with non-fork intervals omitted between successive observations [3].

To isolate structural changes under evolving network conditions, we partition the data by blockchain height into three consecutive segments containing 78, 77, and 77 fork intervals, respectively. This stratification reveals a systematic compression of fork durations over time. All segments exhibit a steep decay, indicating that most forks resolve rapidly, while the presence of a nonzero tail confirms that resolution is not instantaneous but unfolds over a finite, propagation-bounded interval. The late segment shows a markedly faster decay and a substantially reduced tail relative to earlier segments, consistent with improved network propagation and a reduced window for competing discoveries.

While the dependence of fork duration on network conditions has been documented previously [6], our contribution is to reinterpret these observations within an entropy-collapse framework. In this view, proof-of-work competition determines when collapse is initiated, whereas network propagation governs how rapidly collapse is completed in a distributed setting. Bitcoin thereby constructs a coherent and verifiable temporal order without requiring instantaneous global agreement or external synchronization.

B. Implications for Temporal Stability

When the ratio H/D remains approximately constant, the arrival rate implied by the exponential limit remains stable. Under this condition, the system maintains a consistent temporal scale without reference to any external clock. The combination of entropy collapse at the interval scale and mean reversion at the epoch scale implies that a proof-of-work system with stationary fundamentals can function as an autonomous time source. It produces a verifiable sequence of discrete uncertainty-resolving events that can be interpreted consistently by all participants.

This property is particularly relevant in open and distributed environments where no trusted or synchronized external clock

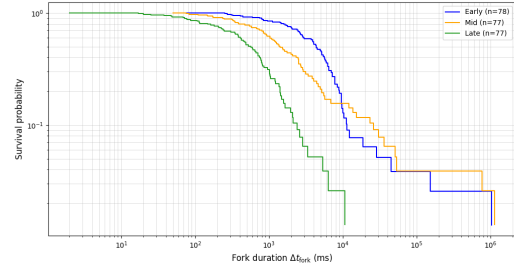


Fig. 5. Empirical Survival Function of Fork Durations Following Block Discovery.

is available. In such settings, time cannot be assumed as a shared input but must be constructed from observable events. An arrival process defined by entropy collapse provides such a mechanism by establishing a common temporal reference through ordered and verifiable events, rather than through dependence on external time authorities. This provides a consistent explanation of Bitcoin’s non-continuous time, both at the level of block discovery and under distributed observation.

V. CONCLUSION

Prior to Bitcoin, Bernoulli and binomial processes were well understood in theory but had not been realized as an open and independently verifiable system operating in the real world. Bitcoin instantiates such a system through probabilistic sampling, cryptographic verification, and adaptive difficulty control. Empirically, global hash trials operate in the Bernoulli limit and produce exponential inter-arrival intervals consistent with Poisson theory. Uncertainty evolves within each interval and is resolved at block discovery, while difficulty adjustment stabilizes the event rate across epochs without suppressing short term randomness. In a distributed network, however, entropy collapse is not completed instantaneously. Empirical observations of temporary forks indicate that residual uncertainty may persist for a short propagation-bounded interval following block discovery before a single history becomes dominant. Together, these results show that Bitcoin maintains a stable yet non-continuous temporal structure without reliance on any unified external clock. More importantly, they illustrate how a permissionless distributed system, in which no trusted reference time can be assumed, can construct a verifiable temporal order endogenously from probabilistic events and protocol-level information.

ACKNOWLEDGMENTS

The author thanks the Bitcoin developer and research communities for making block and difficulty data publicly accessible. Any errors remain the author’s own.

REFERENCES

- [1] B. Chen. Bitcoin: A Non-Continuous Time System. arXiv preprint arXiv:2501.11091, 2025.
- [2] S. Nakamoto. Bitcoin: A Peer-to-Peer Electronic Cash System. 2008. Available: <https://bitcoin.org/bitcoin.pdf>

- [3] C. Decker and R. Wattenhofer. Information propagation in the Bitcoin network. In *IEEE P2P 2013 Proceedings*, pages 1–10, 2013.
- [4] R. Bowden, S. Keil, A. Gervais, S. Matetic, and S. Capkun. Block arrivals in the Bitcoin blockchain. arXiv preprint arXiv:1801.07447, 2018.
- [5] R. Bowden, H. P. Keeler, A. E. Krzesinski, and P. G. Taylor. Modeling and analysis of block arrival times in the Bitcoin blockchain. *Stochastic Models*, 36(4):602–637, 2020.
- [6] T. Neudecker and H. Hartenstein, “An Empirical Analysis of Blockchain Forks in Bitcoin,” in *Financial Cryptography and Data Security (FC 2019)*, pp. 84–92, 2019.
- [7] Bitcoin-data. Bitcoin Block Arrival Time Dataset. Accessed 2025. Available: <https://github.com/bitcoin-data/block-arrival-times>
- [8] S. M. Ross, *Stochastic Processes*. John Wiley and Sons, 1996.
- [9] Bitcoin Core Developers. Bitcoin Core Source Code: Difficulty Adjustment Logic (`src/pow.cpp`). GitHub Repository, 2025. Available: <https://github.com/bitcoin/bitcoin>
- [10] T. M. Cover and J. A. Thomas, *Elements of Information Theory*, John Wiley & Sons, 1999.